Machine Learning Metadynamics for Modeling Drug Release of Phosphoramidate-based Antibody-drug Conjugates in Cancer Treatment

Rizka Nur Fadilla and Yoshitada Morikawa
大阪大学 大学院工学研究科

1. Introduction

Antibody-drug conjugates (ADCs) are biopharmaceutical agents that deliver payloads, such as chemotherapeutic drugs, to cancer cells. The goal is to kill cancer cells while minimizing the damage to healthy cells, which is a common challenge in cancer chemotherapy. This is achieved by conjugating a cytotoxic agent to an antibody via a linker that targets the cancer cells. ADC efficacy depends on antibody specificity, linker cleavage selectivity (stability in the bloodstream but cleavage within cancer cells), and payload potency.[1,2]

Linker instability is a key challenge in the development of the ADC. This instability can cause premature payload release into the bloodstream before reaching the targeted cancer cells. This release can lead to toxicity, as shown by the withdrawal of mylotarg from the market in 2010 [3], following its FDA approval in 2000. Understanding these challenges is essential for successful development of ADCs.

The phosphoramidate-based linker (see Fig. 1) is among the several proposed linkers that address linker instability. It shows stability at neutral pH, corresponding to the extracellular environment, while enabling rapid release under the acidic conditions found in cancer cells. This linker has proven effective in delivering diverse payloads, which could enhance the efficacy of the ADC [4-6]. Despite these promising results, no ADC using this linker has been approved. A possible explanation is the insufficient mechanistic understanding of the payload release.

Exploring the potential energy surface (PES) of chemical reactions is vital for understanding the payload release mechanisms of phosphoramidate-based linkers. PES reveals reaction pathways and energy barriers, helping to optimize linker design and control drug release kinetics. Accurately representing PES requires solving the Schrödinger equation approximated using density functional theory (DFT). However, DFT's computational cost of DFT often limits its application in statistical sampling, such as in metadynamic simulations. [7]

Recent advancements in machine learning methods have demonstrated the capability of accurately modeling the PES when trained accurate data. We developed a machine learning interatomic potential using a Deep Potential method for phosphoramidate in an aqueous environment. This potential was used to investigate the payload release mechanism of the phosphoramidate-based linker.

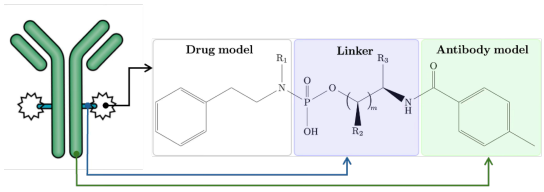

Fig. 1: Components of antibody-drug conjugates with phosphoramidate-based linker. Symbols R_1, R_2, and R_3 denote the substituent of the linker.

2. Computational Method

2.1 Deep Potential

We employed the Deep Potential (DP) framework [8] to construct a machine-learning interatomic potential. In the DP framework, the potential energy is expressed as the sum of atomic energies. Each atomic energy was determined based on the local environment within a specified cutoff radius. This procedure converts the local atomic environment into a descriptor that preserves translational, rotational, and permutational symmetries. The descriptor was fed into a deep neural network to predict the atomic energy and corresponding forces. The neural network was trained on atomic configurations and their corresponding energies and forces using DFT calculations. Once trained, the DP model drove the dynamic simulations. The DP framework was implemented using the DeePMD-kit [9].

2.2 Density-functional Theory (DFT)

Density functional theory (DFT) is a quantum-based approach used to investigate the electronic structures of molecules and materials. DFT-based calculations were used to generate training data for the DP network. CP2K software [10] was employed to compute the energy and atomic forces using revPBE-D2/TZV2P as the exchange-correlation functional/basis set and the GTH pseudopotential [11,12]. The training data comprised two systems: pure bulk water and phosphoramidate in aqueous solution. Fig. 2 and 3 show the typical training structures used in this study.

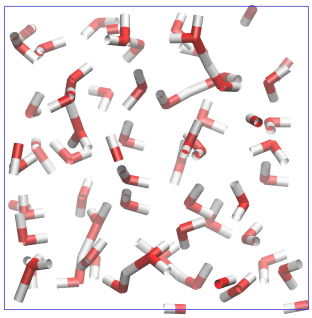

Fig. 2: Pure bulk water. The red and white colors denote oxygen and hydrogen atoms, respectively.

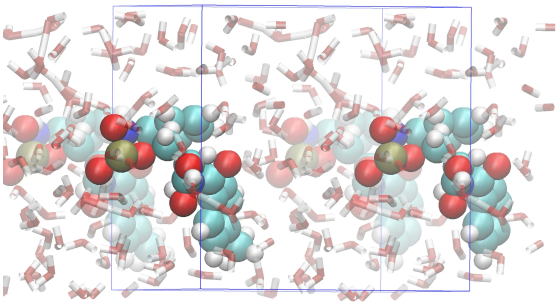

Fig. 3: Phosphoramidate-based ADC in aqueous solution. The red, white, green, blue, and brass colors denote oxygen, hydrogen, carbon, nitrogen, and phosphor atoms.

2.3 Metadynamics

Metadynamics is a simulation technique that accelerates rare-event sampling by introducing a bias potential. This bias potential was applied to the selected collective variables (CVs) that characterized the chemical reaction. In our study, we selected two CVs: the P-N coordination number, reflecting P-N bond cleavage, and the P-O coordination number,

representing P-O bond formation. To perform the metadynamic simulation, we employed Plumed [13] in conjunction with LAMMPS [14].

3. Validation of Deep Potential

To evaluate the accuracy of the developed potential, we compared the machine learning (ML) potential predictions of energy and atomic forces with the results from density functional theory (DFT) (Section 3.1). In addition, we examined the oxygen-oxygen radial distribution function against the experimental results (Section 3.2).

3.1 Energy and Force

Fig. 4 presents parity plots comparing the energy and atomic forces determined by DFT and ML across 5,765 test data points. These test data were excluded from the training process and comprised pure bulk water and phosphoramidate in an aqueous solution. The root mean square errors (RMSE) for energy and atomic forces are 0.63 meV/atom and 67.88 meV/Å, respectively, indicating a high-quality potential.

3.2 Radial Distribution Function

The performance of the ML potential was further corroborated by examining the oxygen-oxygen radial distribution function (RDF) of pure bulk water, as shown in Fig. 5. The deviation between the predicted RDF and experimental data was small. The ML potential predicted a slightly higher localization of water molecules than the experimental observations. This results, along with the parity plot, suggests that our developed ML potential demonstrates a reasonable level of accuracy.

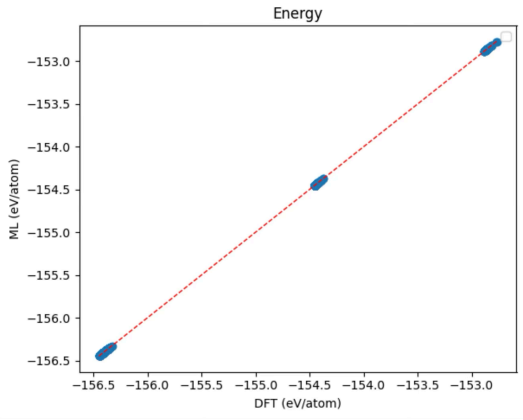

(a)

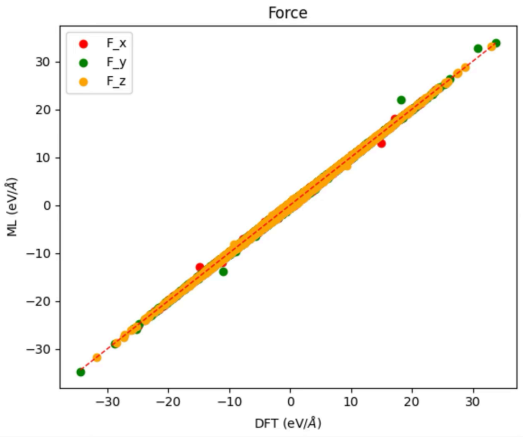

(b)

Fig. 4: Parity plot of (a) energy and (b) atomic forces.

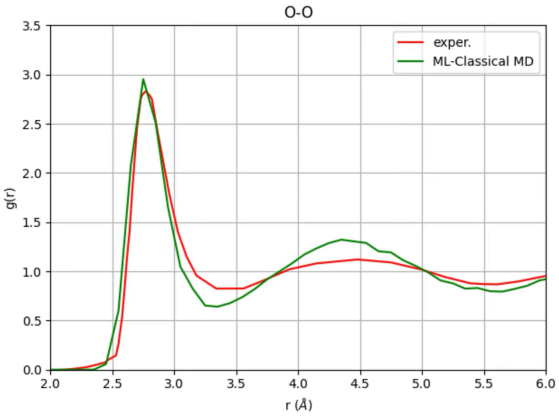

Fig. 5: Oxygen-oxygen radial distribution function of water.

4. P-N hydrolysis

ML metadynamics was employed to simulate the release of payload, which was represented by the cleavage of the P-N bond,

to elucidate the detailed mechanism. In the presence of COOH, it was observed that nitrogen protonation occurred, transitioning from a single N-H coordination to a dual N-H coordination, prior to the cleavage of the P-N bond.[15] This protonation results in slight elongation of the P-N bond, thereby facilitating its cleavage. At neutral pH, COOH tends to deprotonate and exists as COO^- (see Fig. 6). The presence of COO- forms a relatively strong hydrogen bond with the nucleophile H_2O, aiding H_2O in attacking the phosphorus center and promoting P-N bond cleavage. To strengthen our argument, we compared this simulation with one conducted in the absence of COOH, which is currently in progress.

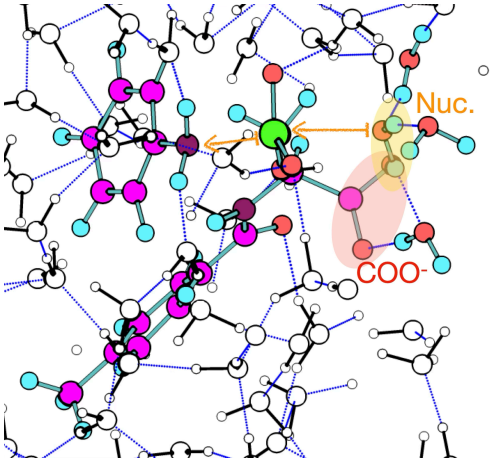

Fig. 6: COO^- assisting the nucleoplhile (Nuc.) H_2O to attack the phosphorus center.

5. Conclusion

We developed a machine learning potential grounded in the Deep Potential framework to model the interatomic interactions of phosphoramidate in aqueous environments. When paired with metadynamic simulations, this potential effectively captures rare events such as payload release through P-N bond cleavage. Our results suggest that in the presence of COOH, nitrogen protonation precedes bond cleavage, and COO^- facilitates nucleophilic attack by stabilizing H_2O near the phosphorus center. Upon completion of this study, we anticipate that the payload release mechanism can be elucidated in detail.

Bibliography

(1) R. V. J. Chari, et al., Angewandte Reviews, **53**, 3751-4005 (2014).

(2) A. Samantasinghar, et al., Biomedicine & Pharmacotherapy, 113308 (2023).

(3) A. D. Ricart, Clinical Cancer Research, **17**, 6417-6472 (2011).

(4) C. J. Choy, et al., Bioconjugate Chemistry, **27**, 824-830 (2016).

(5) C. J. Choy, et al., Bioconjugate Chemistry, **27**, 2206-2213 (2016).

(6) F. P. Olatunji, et al., Bioconjugate Chemistry, **32**, 2386-2396 (2021).

(7) A. Barducci, et al., Wiley Interdisciplinary Reviews: Computational Molecular Science, **1**, 826-843 (2011).

(8) L. Zhang, et al., Physical Review Letters, **120**, 143001 (2018).

(9) H. Wang, et al., Computer Physics Communications, **228**, 178-184 (2018).

(10) T. Kühne, et al., Journal of Chemical Physics, **152**, 194103 (2020).

(11) S. Goedecker, et al., Phys. Rev. B: Condens. Matter Mater. Phys., **54**, 1703 (1996).

(12) C.Hartwigsen, et al., Phys. Rev. B: Condens. Matter Mater. Phys., **58**, 3641 (1998)

(13) G. A. Tiberllo, et al., Computer Physics Communications, **185**, 604 (2014).

(14) A. P. Thompson, et al., Computer Physics Communications, **271**, 10817 (2022).

(15) R. N. Fadilla, et al. Cybermedia HPC Journal, **14,** 89-92 (2024)